

## Kinematic Mechanism of Plasma Electron Hole Transverse Instability

I. H. Hutchinson\*

Plasma Science and Fusion Center, Massachusetts Institute of Technology, Cambridge, Massachusetts 02139, USA

 (Received 16 January 2018; published 17 May 2018)

It is shown through multidimensional particle-in-cell simulations that at least in Maxwellian background plasmas the long-wavelength transverse instability of plasma electron holes is caused not by the previously proposed focusing of trapped particles but instead by kinematic jetting of marginally passing electrons. The mechanism is explained and heuristic analytic estimates obtained which agree with the growth rates and transverse wave numbers observed in the simulations.

DOI: [10.1103/PhysRevLett.120.205101](https://doi.org/10.1103/PhysRevLett.120.205101)

Plasma electron holes are self-sustaining solitonlike structures, in which an electron phase-space deficit on trapped orbits causes a local electric potential maximum that confines those trapped electrons [1]. Spacecraft observations now routinely see these localized electrostatic potential structures in a variety of plasma regions [2–12]. Specific instruments and algorithms are now implemented to detect them, for example on the current magnetospheric multiscale (MMS) mission [13]. Holes are most easily analyzed as vortices in one space and one velocity dimension, but it is known that in three dimensions even holes that start as one-dimensional often break up quickly, by what is called the transverse instability. This effect was observed in the earliest computer simulations of unmagnetized holes [14] and has been confirmed since by many simulation studies [15–22]. It is also known that a strong enough parallel magnetic field can suppress the transverse instability. Despite the importance of the phenomenon, which decides the ultimate structure, persistence, and decay of holes, the transverse instability remains essentially unexplained. It is the purpose of this Letter to identify its underlying mechanism.

Computational simulations [19,23,24] have established approximate quantitative stability criteria sufficient for many purposes, but their interpretation has left open many questions about the mechanism. The present study gives new and more comprehensive simulation results that provide strong evidence *against* the previously proposed mechanism but in favor of a new understanding of the instability mechanism, explained here. It is based on electron hole kinematics: the overall conservation of momentum influenced by “jetting” (a form of energization) of particles by accelerating holes. A full-scale mathematical treatment of the new mechanism is beyond the scope of this Letter.

To avoid confusing the transverse instability caused by holes with the instabilities driven by nonthermal electron distributions, we form a hole (artificially) initially as a one-dimensional slablike structure (the  $y$  and  $z$  coordinates being ignorable). We then observe the growth in two space  $x$  and  $y$  (and three velocity) dimensions of transverse

perturbations. For linear stability purposes, there is no loss of generality in supposing the unstable wave vectors to be chosen along  $y$ , with  $z$  dependence remaining absent.

The particle-in-cell code COPTIC [25], a 3D electrostatic code, is used here as 2D3V, pushing only electrons, the ions being taken as a uniform background. The simulation is initialized with a one-dimensional Schamel-type hole [26] having an initial potential shape of (approximately)  $\phi = \psi \operatorname{sech}^4(x/4)$  (measuring lengths in units of the Debye length  $\lambda_D$ ) for the chosen peak potential  $\psi$  (in units of electron temperature  $T_e/e$ ). Time steps have a length of 0.2 (times the inverse of the plasma frequency  $\omega_p^{-1}$ ). The typical mesh is  $64 \times 128$ . The domain  $-32 < x < 32$  resolves the hole and prevents the open  $x$  boundaries from influencing the instability. Using up to  $-128 < y < 128$  is sufficient to resolve the  $y$  variation of perturbations, as convergence tests with different domain lengths have shown (although not long enough to prove the periodic  $y$  boundaries completely negligible for the longest wavelengths). The transverse velocity distribution and the passing particle distribution are Maxwellian of equal temperature. Typically, 200 million particles are used.

On the basis of their pioneering simulations, Muschietti *et al.* [19,23] proposed a criterion for the parallel magnetic field strength required to suppress the transverse instability: that the electron cyclotron frequency  $\Omega$  exceed the bounce frequency of deeply trapped electrons  $\omega_b$ . For a Schamel hole,  $\omega_b \simeq \omega_p \sqrt{\psi}/2$ . Systematic exploration of the parameter space using COPTIC approximately *confirms* this criterion.

Figure 1 shows the time evolution of the peak potential in a series of two-dimensional simulations. The initial amplitude is given by the value at the left end of the traces ( $t = 0$ ,  $\psi = 0.6, 0.4, 0.2, 0.1, 0.05$ ) where the hole is 1D. Various different magnetic field values (expressed  $\Omega/\omega_p$ ) are used, as shown by the line labels. *Stable* cases preserve the initial value of the peak potential (with some small decay attributable to noise). *Unstable* cases kink and then decrease in  $\psi$  as a nonlinear result. However, unstable cases

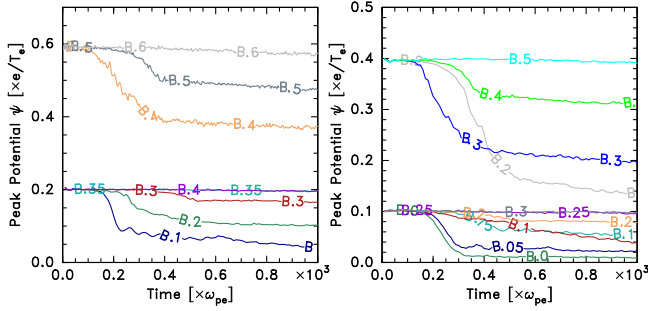


FIG. 1. Evolution with time of the peak potential of electron holes for different magnetic fields.

with magnetic field values not too much below the threshold of instability do not evolve to zero  $\psi$ . Instead, they decrease to a finite value and then continue stably. Values of  $\psi$  below about 0.01 are at approximately the noise level.

The domain of initial stability and instability is shown in Fig. 2(a). On it is plotted the line  $\Omega = \omega_b = \omega_{pe} \sqrt{\psi}/2$ . It can be seen that this estimate of the stability threshold predicts reasonably well the observed stability. However, there is some ambiguity in identifying instability at the marginal level, which appears somewhat to the right of the scaling line.

In view of the apparent self-stabilization of the holes, it is perhaps more interesting to plot the *final* peak potential versus the cyclotron frequency. That is shown in Fig. 2(b), strongly compressing the observed values closer to a single line, thus lending support to the hypothesis that self-stabilization is a matter of reducing the linear growth rate to the threshold. This stabilization threshold line is now more obviously to the right of the  $\Omega = \omega_b$  scaling: by a factor of approximately 1.5.

Based on their observations of the growth of an initial kink, which showed an enhancement of electron density (after “a bounce period”) at the edge of the hole on the *concave* side of an initialized perturbation, Muschietti *et al.* hypothesized that the mechanism of transverse instability was *focusing of trapped electrons* by the kinked hole potential. And they argued that these electron-rich regions were caused by trapped electron motion in the potential

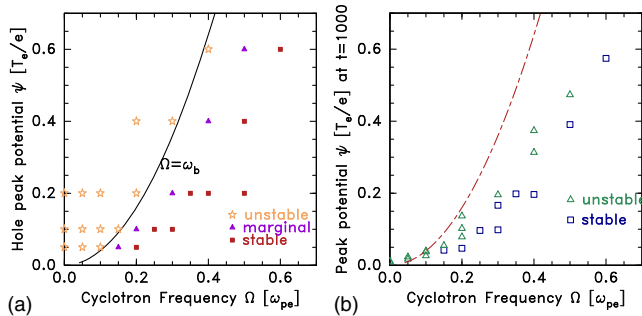


FIG. 2. Domain of stability or instability in respect of the (a) initial hole potential and (b) final hole potential.

well (illustrated in their paper). Their observations were of very deep holes in which the peak hole potential was  $\psi = 1$ , and the potential shape [ $\phi(x)$ , Gaussian] and parallel distribution function were chosen consistently by a Bernstein-Greene-Kruskal integral [1,27] calculation, though anisotropic with a non-Maxwellian passing particle distribution.

Wu *et al.* [24] later used the same hole shape and distribution but grew the transverse instability from noise. They endorsed the focusing interpretation and illustrated that the initial perturbation assumed by Muschietti possesses an electron density enhancement in the concave region, but they did not definitely confirm the existence of charge perturbations of that type in their simulations of the long-wavelength transverse instability. They also observed, especially at higher magnetic field values, waves with a very short transverse wavelength greatly elongated in the parallel direction. Waves like these, seen in various simulations, especially in the regime  $\omega_b < \Omega$ , are often referred to as “whistler” or “streaked” oscillations [20,28,29]. They are different from the long-wavelength transverse instability that is the topic of the present study.

COPTIC results contradict focusing. In them, electron density is not enhanced on the concave side of the curving hole, which was the primary evidence offered to support it. The opposite is usually observed. Figure 3 shows an example: contours of the electron density during a transverse instability where the electron density is enhanced on the convex side of the kinking hole. This happens early in the kinking process, where the perturbation is still linear (as depicted), and persists throughout the growth (for at least the succeeding  $50/\omega_p$  time period) to a strongly nonlinear stage where the hole begins to decay. Convex-side enhancement of the density occurs also in simulations with a finite magnetic field, up to at least  $\Omega/\omega_p = 0.3$ . And although at higher magnetic fields it merges into the noise, no case examined shows a significant concave-side enhancement.

Why the present results are different has not been established, but these observations argue *against* the

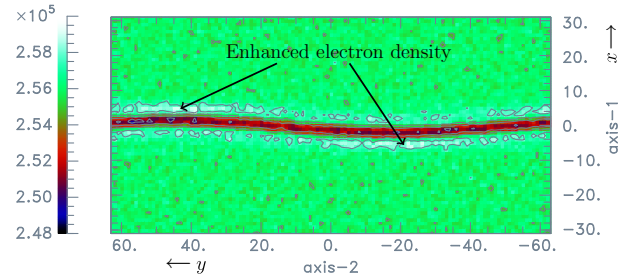


FIG. 3. An example of density (particles per Debye cell) contours in the  $(y, x)$  plane during the early development of the transverse instability. The initial hole peak potential is  $\psi = 0.1T_e/e$ , and no magnetic field is present. The electron density enhancement (lighter shading) in the outer regions adjacent to the hole peak is greater on the convex side.

electron-focusing mechanism Muschietti *et al.* hypothesized to be the general cause of the instability, since the charge supposed to cause it does not occur in the present simulations.

I now explain what I call the *kinematic* mechanism of transverse instability. We have shown [30] that, for 1D holes when the frequency of a perturbation is small compared with the inverse transit time of particles across the hole, there is a jetting effect whereby  $x$  acceleration of a hole (preserving its shape, so that  $\phi(x, t) = \phi_0[x - x_h(t)]$  and  $\ddot{x}_h$  is nonzero) gives rise to a net  $x$ -momentum rate of change,  $\dot{P}$ , of the particles. Because the particle momentum is much larger than the hole field momentum, the sum of the jetting of electrons and ions must be effectively zero. When the ion response is ignorable, which is the case in most of the simulations studying transverse hole instability, the 1D momentum conservation (kinematics) requires  $\dot{P}_e$  to be zero. This is satisfied by a nonaccelerating hole  $\ddot{x}_h = 0$ .

Now consider a 2D situation where the hole center position is given by  $x_h(y, t) = x_a \exp[i(ky - \omega t)]$ , representing a perturbative kink of displacement  $x_a$ . In the absence of any magnetic field, the unperturbed transverse motion of particles (in the direction  $y$ ) is simply a constant velocity  $v_y$ . A growing unstable perturbation has a positive imaginary part of the frequency  $\omega_i$ . If the real part ( $\omega_r$ ) of  $\omega$  is negligible, as it is observed to be in the simulations, a transverse-moving particle still feels an oscillating hole position, because its orbit is  $y = v_y t$  and on it  $x_h(y, t) = x_a \exp(ikv_y t + \omega_i t)$ . We have also recently [31] calculated the effects of hole velocity oscillations at a finite frequency on the jetting of a single particle stream (of ions, but electrons are similar). In summary, there is a coefficient  $K(\omega')$ , arrived at by integrating over the 1D  $v_x$ -distribution function and the hole  $x$  extent, such that a 1D hole that oscillates in position at frequency  $\omega'$  gives  $\dot{P}_e(\omega') = K(\omega')\ddot{x}_h$ . This approach is transferable to particles moving at a specific transverse velocity in a kinked 2D hole by identifying  $kv_y - i\omega_i = \omega'$ . In the limit  $\omega' \rightarrow 0$ ,  $K(\omega')$  tends to a constant value  $K_0$ , and, if a long enough transverse wavelength is considered (small enough thermal  $kv_y$ ),  $K_0$  will apply (to lowest order) to all relevant transverse velocities. Then  $\ddot{x}_h(y, t) = -(kv_y - i\omega_i)^2 x_h$ . When this effect is integrated over a Maxwellian  $v_y$  distribution (symmetric in  $v_y$ ), the imaginary cross term  $kv_y i\omega$  cancels, and we find  $\langle \ddot{x}_h(y, t) \rangle_{v_y} = (-\langle kv_y \rangle_{v_y} + \omega_i^2) x_a = (-k^2 T_y / m_e + \omega_i^2) x_a$ , so  $\dot{P}_e = (\omega_i^2 - k^2 T_y / m_e) K_0 x_a$ .

Since the momentum balance is  $\dot{P}_e = 0$ , it does not actually matter what the magnitude of  $K_0$  is (so long as it has its low-frequency sign). We deduce that the kink growth rate is

$$\gamma = \omega_i = \pm k \sqrt{\frac{T_y}{m_e}}. \quad (1)$$

This, I propose, is the *transverse instability* at low  $k$ . It has nothing to do with transverse focusing.

The heuristic explanation of the transverse instability is simple. For a single  $v_y$ , it is that the combination of the apparent  $x$  acceleration of the hole in the particle's transverse frame of reference, arising because of the kinked hole's curvature [the  $(kv_y)^2$  term], is exactly canceled by the actual acceleration of the hole in the kink's  $y$ -position rest frame, represented by the growth of the kink: ( $\omega_i^2$ ). So the electron of velocity  $v_y$  sees zero total hole acceleration and experiences no jetting.

If the transverse wave number is increased, then eventually  $kv_y$  and, hence,  $\omega'$  become comparable to the parallel electron transit time, and the coefficient  $K(\omega')$  decreases in the real part (and acquires an imaginary part; see Fig. 4 in Ref. [31]). Heuristically, when a reversal of  $\mathcal{R}(K)$  occurs for the majority of the particles responsible for jetting, so that the sign of  $P$  is reversed, the instability is suppressed. Our prior kinematic analysis (Sec. IIID in Ref. [30]) showed that for  $\psi < 1$  the parallel velocity extent of the particles responsible for jetting is approximately  $\sqrt{\psi}$ . Particles up to that velocity have a transit time of approximately  $L/\sqrt{\psi}$ , where  $L$  is the hole  $x$  length: equal to roughly 4 (Debye lengths). We may therefore estimate the wave number at which  $\mathcal{R}[K(\omega')] \simeq 0$  will occur as being where  $\omega' L / \sqrt{\psi} \simeq 1$ . Substituting a thermal transverse velocity  $v_y = 1$ , we get an estimate for the cutoff wave number for full stabilization:  $k_c \simeq \sqrt{\psi} / L$ .

Since for small  $k$  the growth rate  $\omega_i$  is proportional to  $k$ , there must be a maximum growth rate somewhere below  $k_c$ , perhaps at approximately half  $k_c$ , and having a rate perhaps half the linear extrapolation. Thus, we estimate the maximum growth rate as  $\gamma \simeq k_c / 4 \simeq \sqrt{\psi} / 4L \sim \sqrt{\psi} / 16$  in units of  $\omega_p$ .

In order to test the scaling expected from the kinematic analysis of the transverse instability, a series of runs was carried out over a systematic range of hole depths from  $\psi = 0.05$  to  $2T_e/e$ . Figure 4 shows the results. The growth rate is found by fitting an exponential to the systematically rising part of the mode amplitude measured in two ways whose difference indicates approximately the uncertainty (error bars). The  $k$  values are determined by finding the mean mode number of the dominant mode, treated either by finding the centroid of (one side of) the absolute value of the Fourier transform of  $x(y)$  or by interpolating only at the largest mode and those adjacent to it (peaked). Again, the two values are indicative of the uncertainties.

The results agree with expectations. Both  $\gamma$  and  $k$  scale approximately proportional to  $\sqrt{\psi}$ . The observed absolute values of growth rate  $\gamma$  are of the same order of magnitude as  $k$  but not exactly equal to it. Equality would be expected only for  $k \ll k_c$ . But the simulation is presumably dominated by the peak growth rate at which we have estimated

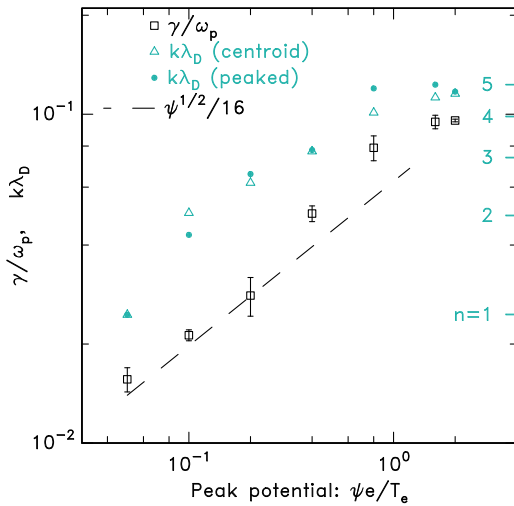


FIG. 4. Growth rate  $\gamma$  and wave number  $k$  (in natural normalized units) observed for the transverse instability as a function of the hole peak potential (depth)  $\psi$ . The number of wavelengths in the computational domain is indicated at the right  $n = 1, 2, \dots$

$\gamma \simeq k/2$ , which agrees with observations. The absolute value of  $\gamma$  is quite close to the estimate  $\sqrt{\psi}/16$ .

The kinematic mechanism worked out here takes the magnetic field to be negligibly small, although it will also apply at nonzero parallel magnetic fields of low magnitude. The higher fields that lead to stabilization of the transverse instability require accounting for the electrons' helical orbits. Heuristically, one might suppose that, when the cyclotron period becomes short enough compared to the transit time (and, hence, the Larmor radius small compared with the Debye length), the destabilizing effects of transverse motion will be suppressed. But a rigorous mathematical treatment well beyond the present analysis is essential both to show how full stabilization occurs and to determine the precise value of the criterion. (This analysis has now been undertaken by the author and will be published elsewhere. It confirms the results of the present Letter.) Previous mathematical analyses [32,33] have been misled by adopting a symmetric potential eigenmode as a first approximation and expanding in inverse powers of frequency. In all simulations, the observed eigenmode is approximately a shift: an antisymmetric mode; and the kinematic effect is strongest at a low frequency, so the expansion is inappropriate. Note though that the magnetic stabilization criterion being expressible in terms of the bounce frequency is *not* a demonstration that *trapped* particles are responsible for the instability, because the significant *passing* particles' transit frequency approximates the minimum bounce frequency.

Despite exploring a wide parameter range, the present simulations with isotropic Maxwellian background distributions *never* gave rise to the whistler or streaked waves. However, such phenomena do occur in COPTIC simulations with anisotropic temperature  $T_{\perp} > T_{\parallel}$  and can readily

cause a breakup of holes in those situations. I interpret these facts tentatively as an indication that these different phenomena are most probably (in COPTIC simulations *certainly*) instabilities provoked by the background plasma distribution. They might be important for holes in nature but depend upon the details of the plasma through which they are passing and are not the intrinsic transverse instability.

I am grateful to Chuteng Zhou, for many helpful discussions. This work was partially supported by NASA Grant No. NNX16AG82G. Computer simulations were carried out on the MIT PSFC parallel AMD Opteron/Infiniband cluster Loki and on the MIT-PSFC partition of the Engaging cluster at the MGHPCC facility [34], which was funded by DOE Grant No. DE-FG02-91-ER54109.

\*ihutch@mit.edu

- [1] I. H. Hutchinson, Electron holes in phase space: What they are and why they matter, *Phys. Plasmas* **24**, 055601 (2017).
- [2] H. Matsumoto, H. Kojima, T. Miyatake, Y. Omura, M. Okada, I. Nagano, and M. Tsutsui, Electrostatic solitary waves (ESW) in the magnetotail: BEN wave forms observed by GEOTAIL, *Geophys. Res. Lett.* **21**, 2915 (1994).
- [3] R. E. Ergun, C. W. Carlson, J. P. McFadden, F. S. Mozer, L. Muschietti, I. Roth, and R. J. Strangeway, Debye-Scale Plasma Structures Associated with Magnetic-Field-Aligned Electric Fields, *Phys. Rev. Lett.* **81**, 826 (1998).
- [4] S. D. Bale, P. J. Kellogg, D. E. Larsen, R. P. Lin, K. Goetz, and R. P. Lepping, Bipolar electrostatic structures in the shock transition region: Evidence of electron phase space holes, *Geophys. Res. Lett.* **25**, 2929 (1998).
- [5] A. Mangeney, C. Salem, C. Lacombe, J.-L. Bougeret, C. Perche, R. Manning, P. J. Kellogg, K. Goetz, S. J. Monson, and J.-M. Bosqued, WIND observations of coherent electrostatic waves in the solar wind, *Ann. Geophys.* **17**, 307 (1999).
- [6] J. Pickett, L.-J. Chen, R. Mutel, I. Christopher, O. Santolk, G. Lakhina, S. Singh, R. Reddy, D. Gurnett, B. Tsurutani, E. Lucek, and B. Lavraud, Furthering our understanding of electrostatic solitary waves through Cluster multispacecraft observations and theory, *Adv. Space Res.* **41**, 1666 (2008).
- [7] L. Andersson, R. E. Ergun, J. Tao, A. Roux, O. LeContel, V. Angelopoulos, J. Bonnell, J. P. McFadden, D. E. Larson, S. Eriksson, T. Johansson, C. M. Cully, D. L. Newman, M. V. Goldman, K. H. Glassmeier, and W. Baumjohann, New Features of Electron Phase Space Holes Observed by the THEMIS Mission, *Phys. Rev. Lett.* **102**, 225004 (2009).
- [8] L. B. Wilson, C. A. Cattell, P. J. Kellogg, K. Goetz, K. Kersten, J. C. Kasper, A. Szabo, and M. Wilber, Large-amplitude electrostatic waves observed at a supercritical interplanetary shock, *J. Geophys. Res.* **115**, A12104 (2010).
- [9] D. M. Malaspina, D. L. Newman, L. B. Willson, K. Goetz, P. J. Kellogg, and K. Kersten, Electrostatic solitary waves in the solar wind: Evidence for instability at solar wind current sheets, *J. Geophys. Res.* **118**, 591 (2013).
- [10] D. M. Malaspina, L. Andersson, R. E. Ergun, J. R. Wygant, J. W. Bonnell, C. Kletzing, G. D. Reeves, R. M. Skoug, and

- B. A. Larsen, Nonlinear electric field structures in the inner magnetosphere, *Geophys. Res. Lett.* **41**, 5693 (2014).
- [11] I. Y. Vasko, O. V. Agapitov, F. Mozer, A. V. Artemyev, and D. Jovanovic, Magnetic field depression within electron holes, *Geophys. Res. Lett.* **42**, 2123 (2015).
- [12] F. S. Mozer, O. A. Agapitov, A. Artemyev, J. L. Burch, R. E. Ergun, B. L. Giles, D. Mourenas, R. B. Torbert, T. D. Phan, and I. Vasko, Magnetospheric Multiscale Satellite Observations of Parallel Electron Acceleration in Magnetic Field Reconnection by Fermi Reflection from Time Domain Structures, *Phys. Rev. Lett.* **116**, 145101 (2016).
- [13] D. M. Malaspina, A. Ukhorskiy, X. Chu, and J. Wygant, *J. Geophys. Res.: Space Phys.* (to be published).
- [14] R. L. Morse and C. W. Nielson, One-, Two-, and Three-Dimensional Numerical Simulation of Two-Beam Plasmas, *Phys. Rev. Lett.* **23**, 1087 (1969).
- [15] F. Mottez, S. Perraut, A. Roux, and P. Louarn, Coherent structures in the magnetotail triggered by counterstreaming electron beams, *J. Geophys. Res.* **102**, 11399 (1997).
- [16] T. Miyake, Y. Omura, H. Matsumoto, and H. Kojima, Two-dimensional computer simulations of electrostatic solitary waves observed by Geotail spacecraft, *J. Geophys. Res.* **103**, 11841 (1998).
- [17] M. V. Goldman, M. M. Oppenheim, and D. L. Newman, Nonlinear two-stream instabilities as an explanation for auroral bipolar wave structures, *Geophys. Res. Lett.* **26**, 1821 (1999).
- [18] M. Oppenheim, D. L. Newman, and M. V. Goldman, Evolution of Electron Phase-Space Holes in a 2D Magnetized Plasma, *Phys. Rev. Lett.* **83**, 2344 (1999).
- [19] L. Muschietti, I. Roth, C. W. Carlson, and R. E. Ergun, Transverse Instability of Magnetized Electron Holes, *Phys. Rev. Lett.* **85**, 94 (2000).
- [20] M. M. Oppenheim, G. Vetoulis, D. L. Newman, and M. V. Goldman, Evolution of electron phase-space holes in 3D, *Geophys. Res. Lett.* **28**, 1891 (2001).
- [21] N. Singh, S. M. Loo, and B. E. Wells, Electron hole structure and its stability depending on plasma magnetization, *J. Geophys. Res.* **106**, 21183 (2001).
- [22] Q. M. Lu, B. Lembege, J. B. Tao, and S. Wang, Perpendicular electric field in two-dimensional electron phase-holes: A parameter study, *J. Geophys. Res.* **113**, A11219 (2008).
- [23] L. Muschietti, I. Roth, R. E. Ergun, and C. W. Carlson, Analysis and simulation of BGK electron holes, *Nonlinear Processes Geophys.* **6**, 211 (1999).
- [24] M. Wu, Q. Lu, C. Huang, and S. Wang, Transverse instability and perpendicular electric field in two-dimensional electron phase-space holes, *J. Geophys. Res.* **115**, A10245 (2010).
- [25] I. H. Hutchinson, Forces on a Small Grain in the Nonlinear Plasma Wake of Another, *Phys. Rev. Lett.* **107**, 095001 (2011).
- [26] H. Schamel, Electron holes, ion holes and double layers: Electrostatic phase space structures in theory and experiment, *Phys. Rep.* **140**, 161 (1986).
- [27] I. B. Bernstein, J. M. Greene, and M. D. Kruskal, Exact nonlinear plasma oscillations, *Phys. Rev.* **108**, 546 (1957).
- [28] D. L. Newman, M. V. Goldman, M. Spector, and F. Perez, Dynamics and Instability of Electron Phase-Space Tubes, *Phys. Rev. Lett.* **86**, 1239 (2001).
- [29] M. Berthomier, L. Muschietti, J. W. Bonnell, I. Roth, and C. W. Carlson, Interaction between electrostatic whistlers and electron holes in the auroral region, *J. Geophys. Res.* **107**, SMP 26-1 (2002).
- [30] I. H. Hutchinson and C. Zhou, Plasma electron hole kinematics. I. Momentum conservation, *Phys. Plasmas* **23**, 082101 (2016).
- [31] C. Zhou and I. H. Hutchinson, Plasma electron hole oscillatory velocity instability, *J. Plasma Phys.* **83**, 905830501 (2017).
- [32] H. Schamel, Stability of Electron Vortex Structures in Phase Space, *Phys. Rev. Lett.* **48**, 481 (1982).
- [33] D. Jovanović and H. Schamel, The stability of propagating slab electron holes in a magnetized plasma, *Phys. Plasmas* **9**, 5079 (2002).
- [34] <http://www.mghpcc.org>.